Journal of Biochemical and Biophysical Methods, 1 (1979) 195—208

THE MEASUREMENT OF SUBNANOSECOND FLUORESCENCE DECAY OF FLAVINS USING TIME-CORRELATED PHOTON COUNTING AND A MODE-LOCKED Ar ION LASER

A.J.W.G. VISSER [1] and A. VAN HOEK [2]

[1] *Department of Biochemistry, Agricultural University, De Dreijen 11, 6703 BC Wageningen, and* [2] *Laboratory of Molecular Physics, Agricultural University, De Dreijen 6, 6700 EP Wageningen, The Netherlands*

(Received 8 March 1979; accepted 27 March 1979)

A system is described consisting of a mode-locked Ar ion laser and time-resolved photon-counting electronics. The system is capable of measuring fluorescence lifetimes in the subnanosecond time domain. The Ar ion laser is suitable for the excitation of flavins, since the available laser wavelengths encompass the first absorption band of the yellow chromophore. Due to the high radiation density and the short pulse, both the time and wavelength resolution of the fluorescence of very weakly emitting compounds can be measured. Experiments have been described for flavin models exhibiting single and multiple modes of decay. In these examples lifetimes were determined both from deconvolved decay curves and from direct analysis of the tail of the curve, where no interference of the exciting pulse is encountered. Both determinations showed very good agreement. Due to the highly polarized laser light the decay of the emission anisotropy could be measured directly after the exciting pulse. In principle, fast rotational motions might be detected. An anisotropy measurement conducted with a flavoprotein with a noncovalently attached FAD is presented.

Key words: mode-locked laser; flavins; fluorescence decay; emission anisotropy.

INTRODUCTION

The fluorescence of flavins is strongly influenced by interactions with aromatic or electron-rich molecules, which are in close proximity to the yellow chromophore. The dynamic part of these interactions gives rise not only to a decrease of the fluorescence efficiency, but also to a drastic shortening of the fluorescence lifetime [1—3]. When the flavin is only surrounded by solvent molecules the measured lifetimes are in order of 4—10 ns depending on the conditions employed [4]. These rather long lifetimes can easily be determined due to the high quantum yield of the fluorescence. On the other hand, the fluorescence perturbed by interacting groups has lost con-

Abbreviations: FWHM, full width at half-maximum; CW, continuous wave; MCA, multichannel analyzer; PMT, photomultiplier; TAC, time-to-amplitude converter.

siderable intensity and is characterized by time constants sometimes in the subnanosecond time domain [2]. In order to obtain accurate dynamic information we used a mode locked Ar ion laser as excitation source. This type of laser provides short pulses (FWHM less than 100 ps) of high radiation energy, at wavelengths in the blue spectral region. This is in perfect coincidence with the red portion of the lowest absorption band of the flavin. In this paper the results of the decay measurements are presented that were conducted with suitable model compounds, namely 3,7,8,9,10-pentamethylisoalloxazine in water with and without the presence of the collisional quencher potassium iodide and a flavinyltryptophan peptide [4,5]. The virtually 100% linearly (vertically) polarized laser light permits one to obtain the decay of the emission anisotropy directly after the pulse from which in principle rapid rotational motion of the bound flavin in flavoproteins can be monitored. Experiments of this type are described with the flavin bound as cofactor FAD to the enzyme lipoamide dehydrogenase [6].

MATERIALS AND EQUIPMENT

Materials

3,7,8,9,10-Pentamethylisoalloxazine was synthesized according to Grande et al. [7]. The N(3)-substituted flavinyltryptophan methyl ester peptide was prepared according to Föry et al. [8]. Lipoamide dehydrogenase (EC 1.6.4.3) was purified from pig heart as described by Massey et al. [9]. Erythrosine B was purchased from Eastman Kodak and was used as received. All reagents used were of analytical grade and buffers were made from doubly distilled water.

Instruments

Absorption spectra were obtained with a Cary 14 spectrophotometer and fluorescence spectra were recorded on an Aminco SPF-500 spectrofluorometer. The laser system and associated optical and electronical components are schematically depicted in Fig. 1. The laser is a Coherent Radiation Model CR 18 UV Ar ion laser. The mode-locking acousto-optic element is a brewster prism (Harris Corp.), driven by a 38 070 MHz signal from the frequency synthesizer ND 60 M from Schomandl. The different lines at 514.4, 501.7, 496.5, 476.7, 472.7 and 457.9 nm can be mode locked individually. In the present study the 476.7 nm line was used. The 76 140 MHz optical pulses were monitored with a fast photodiode and a sampling oscilloscope (Hewlett Packard 1430C, 1811A, 181A). The measured total FWHM was about 180 ps. It can be expected that the FWHM of the light pulse is less than 100 ps when corrected for the rise time of the detector. At 25 A laser discharge current the output of the laser was about 400 mW (CW) and about 100 mW of averaged mode locked power. With beam splitters about 0.5—2 mW of

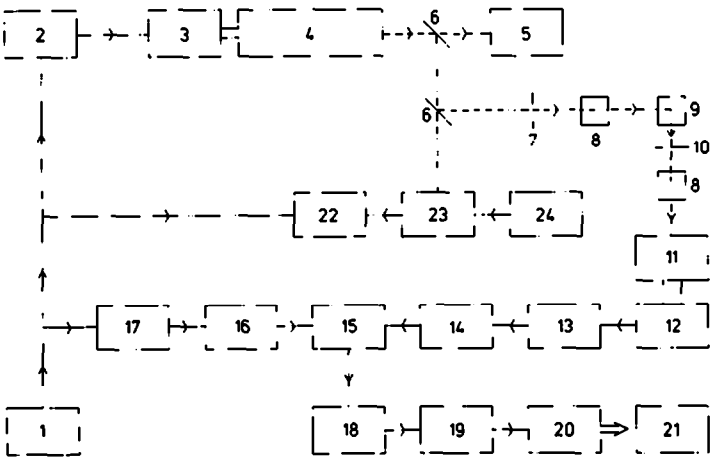

Fig. 1. Block diagram of the experimental set-up. 1, frequency synthesizer; 2, variable gain amplifier; 3, acousto-optic modulator; 4, Ar ion laser; 5, power meter; 6, beam splitter; 7, variable density filter; 8, optical polarizer; 9, sample cuvet; 10, cut-off filter; 11, monochromator or interference filter; 12, photomultiplier; 13, fast amplifier; 14, constant fraction discriminator; 15, time-to-amplitude converter; 16, 100 MHz discriminator; 17, variable time delay; 18, analog to digital converter; 19, multichannel analyzer; 20, cassette tape deck; 21, computer; 22, sampling oscilloscope; 23, fast photodiode; 24, bias supply.

averaged mode locked power were deflected towards the sample compartment. The detection photomultiplier (PMT) is a Philips XP2020 placed in a thermoelectric-cooled housing of Products of Research Inc. in order to reduce background noise. The electronical part consists of modules of the Ortec 9200 system and of a Laben model 8001 multichannel analyzer (MCA). The time scale was calibrated by an Ortec model 462 time calibrator. Because of the very inefficient use of information when the time-to-amplitude converter (TAC) is started with the very high frequency of the laser light pulses, the start and stop channels were reversed [10] (dead time of the TAC is 5 μs). The TAC was started with an emission photon pulse and stopped with a trigger pulse, initiated by the 38 070 MHz signal of the synthesizer. Scattering from glycogen solutions and fluorescence data were collected at a constant starting rate of about 25 kHz. For the scatter solution the exciting beam was additionally attenuated to 1—2 μW averaged mode-locked power with neutral density filters (Balzers). To eliminate effects of rotational motion on the lifetimes, a polarizer (Polacoat) was placed at 55° with respect to the vertical in front of the monochromator (Jarrell Ash 82410, band width 6 nm) in the detection light path [11].

The polarizers used for the emission anisotropy measurements were Glan Thompson prisms. The polarized emission components ($i_{\parallel}(t)$ and $i_{\perp}(t)$) were viewed through a Schott KV 520 cut-off filter and a Balzers 554 nm interference filter. The polarizer in the detection light path is clamped in a motor-driven rotatable mount and can be rotated over 90° and back by applying

logic pulses to an activating relay. By using the timer of the MCA for supply of the logic pulses it is possible to measure $i_{\parallel}(t)$ and $i_{\perp}(t)$ alternately during a preset time and to store the results into two memory subgroups. The instrumental response function was obtained in the same way from a diluted glycogen scattering solution replacing the sample under investigation. The filters in the detection light path were removed. Since the scattered light from glycogen solutions is highly polarized (>95%) only $i_{\parallel}(t)$ of the scatter solution was employed in subsequent deconvolution procedures.

METHODOLOGY

Data analysis

In order to account for the finite duration of the exciting pulse in the analysis of the complete decay curve one has to rely on deconvolution procedures. We used the nonlinear least-squares method for deconvolution of the fluorescence decay [12]. Some data were also analyzed with a response function ($g(t)$) obtained from a quantum counter in order to check the wavelength dependence of the detector [13]. A suitable quantum counter for the flavin system is erythrosine B in water since it has a very short lifetime of about 90 ps [14].

Polarized decay data were analyzed as described by Dale et al. [15]. Multiplication factors in order to correct for imperfect polarizers were obtained as follows [15,16]. The decay profiles of $i_{\parallel}(t)$ and $i_{\perp}(t)$ of a fluorescent solution were semi-simultaneously collected in two different halves of the MCA memory. After correcting for background, the integrals of $i_{\parallel}(t)$ and $i_{\perp}(t)$ over N channels were determined. In a separate experiment the steady-state degree of polarization (p) was accurately measured [6]. All subsequent curves ($i_{\perp}(t)$) were multiplied with the following normalization factor:

$$N_0 = \frac{1-p}{1+p} \frac{\int_0^T i_{\parallel}(t)\,\mathrm{d}t}{\int_0^T i_{\perp}(t)\,\mathrm{d}t} \tag{1}$$

where T is the last point of the decay curve in the MCA.

Sum and difference decays, determined from $i_{\parallel}(t)$ and $i_{\perp}(t)$, can be considered as convolution products:

$$s(t) = i_{\parallel}(t) + 2i_{\perp}(t) = \int_0^t g(t-t')S(t')\,\mathrm{d}t'$$

$$\mathrm{d}(t) = i_{\parallel}(t) - i_{\perp}(t) = \int_0^t g(t-t')D(t')\,\mathrm{d}t' \tag{2}$$

Whenever necessary the total fluorescence $s(t)$ can be analyzed in a sum of exponential terms:

$$S(t) = \sum_{i=1}^{n} \alpha_i \, e^{-t/\tau_i} \tag{3}$$

the parameters were obtained after a search for the minimum value of χ^2 (cf. legend of Fig. 3).

The anisotropy decay $r(t)$ follows from

$$r(t) = \frac{d(t)}{s(t)} \tag{4}$$

Usually $r(t)$ is written as

$$r(t) = \sum_{i=1}^{n} \beta_i \, e^{-t/\phi i} \tag{5}$$

where n is equal to either 1 or 2, ϕ_i is the correlation time for the decay of the anistotropy, β_i the preexponential factor and $\Sigma_{i=1}^{n}\beta_i$ the anisotropy at time zero. As pointed out by Dale et al., $r(t)$ can be obtained from deconvolution of the difference decay according to two models [15]:

(1) The multiexponential character of $s(t)$ arises from microheterogeneity of the fluorophore (different environments giving rise to different lifetimes) in which the difference decay is analyzed from

$$d(t) = \sum_{i=1}^{n} r_i(t)s_i(t) \tag{6}$$

where i indicates the individual species.

(2) There exists rotational anisotropy in a single environment from which $d(t)$ is computed as the following convolution product:

$$d(t) = r(t) \times S(t) = g(t) \times (\sum_{i=1}^{n} \beta_i \, e^{-t/\phi_i})(\sum_{i=1}^{m} \alpha_i \, e^{-t/\tau_i}) \tag{7}$$

In principle the decay of the anisotropy can be derived from the sum and difference decay curves (Eqns. 2 and 4) and analysis can be performed directly without reference to the two models.

Emission spectra

In Fig. 2 normalized spectra are shown from the compounds used in this work. The wavelengths of excitation and emission employed in the decay experiments as well as that of the expected Raman line of water are also indicated in the figure.

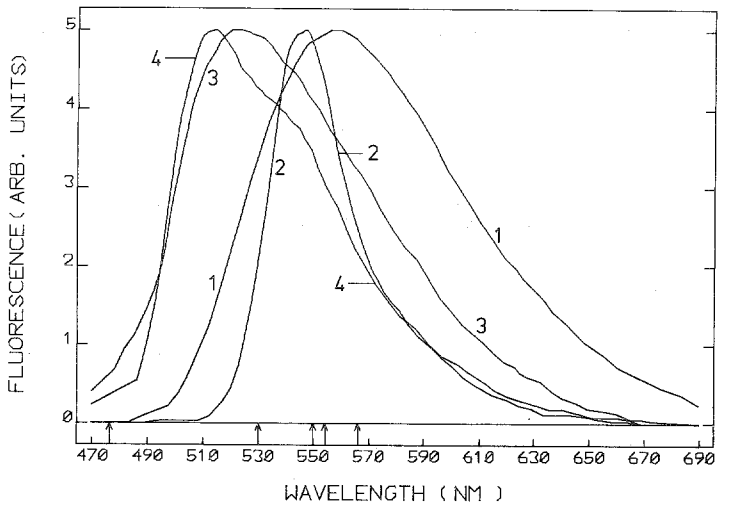

Fig. 2. Peak normalized emission spectra of the compounds used in this work. Excitation wavelength was 476 nm. Optical densities were adjusted to 0.05 at 476 nm. (1) 3,7,8,9,-10-pentamethylisoalloxazine in 50 mM sodium phosphate, pH 7.0; (2) erythrosine B in 50 mM sodium phosphate pH 7.0; (3) *N*(3)-flavinyltryptophan methyl ester in 50 mM sodium phosphate pH 7.0; (4) lipoamide dehydrogenase in 30 mM sodium phosphate/0.3 mM EDTA pH 7.2. Starting from the shortest wavelength the four arrows indicate respectively the exciting wavelength (476 nm), the emission wavelength (530 nm) in case of the peptide, the observation wavelengths (550 and 554 nm) for the model flavin, erythrosine B and lipoamide dehydrogenase and the expected Raman line of water (568.9 nm) when excitation is at 476.7 nm.

Examples

As an example of the range of lifetimes that can be measured the decay profiles of aqueous solutions of scatter (glycogen), erythrosine B and 3,7,8,9,10-pentamethylisoalloxazine (quenched with KI) are presented in Figs. 3A and B. The convoluted curves and the deviation functions of the residuals are also shown *. The single photon data were collected during a fixed period of a multiple of 100 s to accumulate at least 40 000 counts in the maximum. Background collected during the same period of time was subtracted from the decay curve. The scattered laser light pulse as seen by the detection system has a FWHM of 500—600 ps. The reason is that the excitation pulse is broadened in time by transit time variations in the PMT and broadened and somewhat distorted by time walk in the constant fraction-timing discriminator. In case of unquenched or partly quenched

* The exact nature of the oscillation, which becomes manifest in the deviation curve, is not known. The oscillation spoils the χ^2 value, but does not appear to effect the reproducibility of the parameter values. The standard deviation of the parameters was always less than the most significant digit in the reported values.

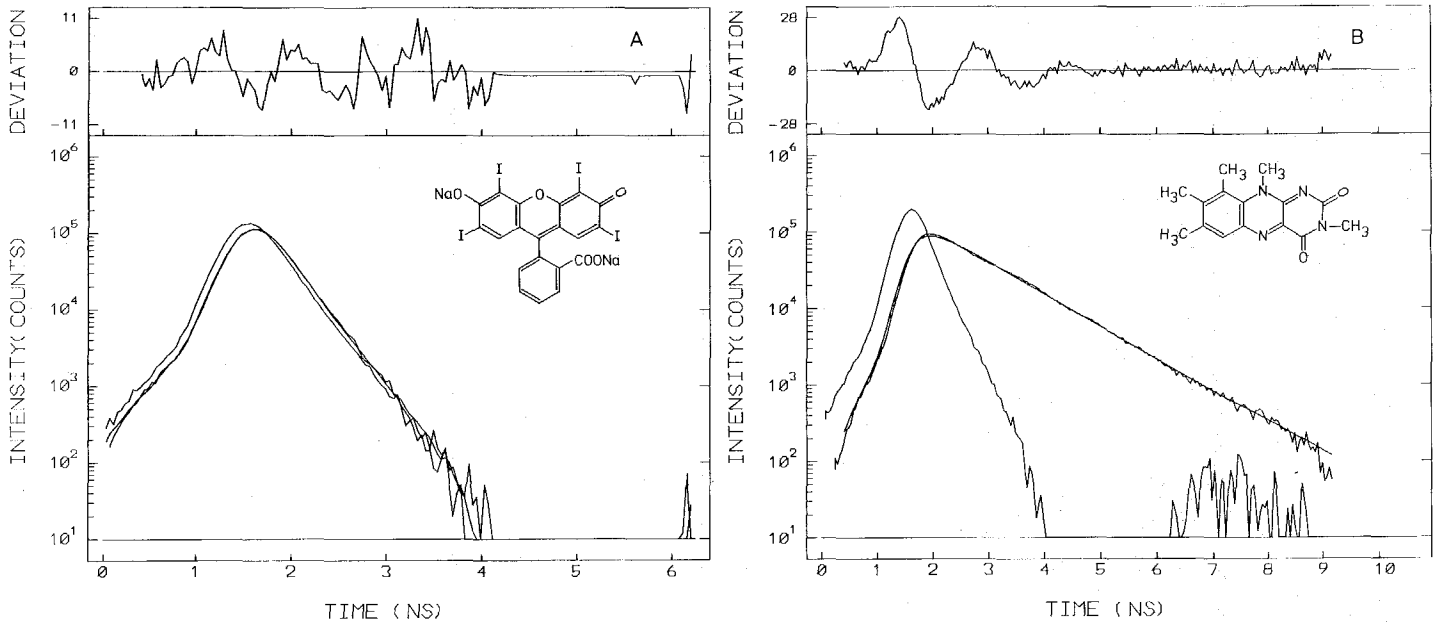

Fig. 3. Fluorescence decay curves of the model compounds used. Excitation profiles ($g(t)$), experimental ($F(t)$) and calculated ($F_c(t)$) decay curves are shown. F_c is the result of a convolution of $g(t)$ with a single exponential function. The deviation function ($DV(i)$) of the weighted residuals in each channel i is displayed on top of the decay curves.

$$DV(i) = (F(i) - F_c(i))/\sqrt{F(i)}; \quad \chi^2 = \frac{1}{N}\sum_{i=1}^{N}\frac{(F(i) - F_c(i))^2}{F(i)};$$

N = number of channels used in the MCA. A, erythrosine B in 50 mM sodium phosphate pH 7.0; τ = 80.2 ps; χ^2 = 11. B, 3,7,8,9,10-pentamethylisoalloxazine in 50 mM sodium phosphate pH 7.0 quenched with 45 mM KI; τ = 1.01 ns; χ^2 = 64.

flavin fluorescence, the tail of the decay curve can be analyzed directly without taking the finite width of the exciting pulse into account. The data obtained from the rapidly decaying samples required deconvolution to extract the correct time constant(s). The fluorescence of erythrosine B is completely relaxed within the time lapse between two laser pulses, therefore analysis has to be performed across the whole decay profile. In fact, the fluorescence response appears as an exciting pulse profile a few channels shifted in time with respect to the impulse response (see Fig. 3A). From three independent measurements the time constant of erythrosine B is 88 ± 10 ps in accordance with the reported values of 90, 110 and 57 ps (see references in ref. 14). In order to investigate the wavelength dependence of the detector 3,7,8,9,10-pentamethylisoalloxazine can be employed as a convenient standard having one single lifetime [4]. The data can be analyzed using the following impulse response functions:

(1) The laser pulse measured with a scatter solution at the exciting wavelength.

(2) The pulse determined at the emission wavelength using a compound with a well determined single short lifetime (erythrosine B: τ = 88 ps).

(3) The pulse measured at the exciting wavelength, but purposely shifted over a certain fraction of time [17].

We determined the lifetime of 3,7,8,9,10-pentamethylisoalloxazine in water using the three different response functions in the convolution procedure. Neither a positive nor a negative shift in time of the excitation pulse gives an improvement of the quality of the fit. As judged from the deviation function and the constant χ^2 values it is to be noted that the first two methods all lead to the same mono-exponential lifetimes. All results obtained with the quenched and unquenched 3,7,8,9,10-pentamethylisoalloxazine are collected in Table 1.

TABLE 1

DYNAMIC FLUORESCENCE QUENCHING OF 3,7,8,9,10-PENTAMETHYLISOALLOXAZINE

The compound (10 μM) was dissolved in 0.1 M sodium phosphate, pH 7.0 Quencher (KI) was added from a 3 M stock solution in water.

Concentration of quencher (mM)	τ [a] (ns)	τ_0/τ	F_0/F [b]
0.0	1.72 (1.73)	1.00	1.00
45	1.01 (1.00)	1.73	2.04
150	0.52 (0.51)	3.39	5.14

[a] Results from a one component analysis. The values between brackets were obtained from analysis of the tail of the decay curve starting at about 2.5 ns after the excitation maximum (cf. Fig. 3B).

[b] Fluorescence intensity ratio obtained by comparing peak maxima.

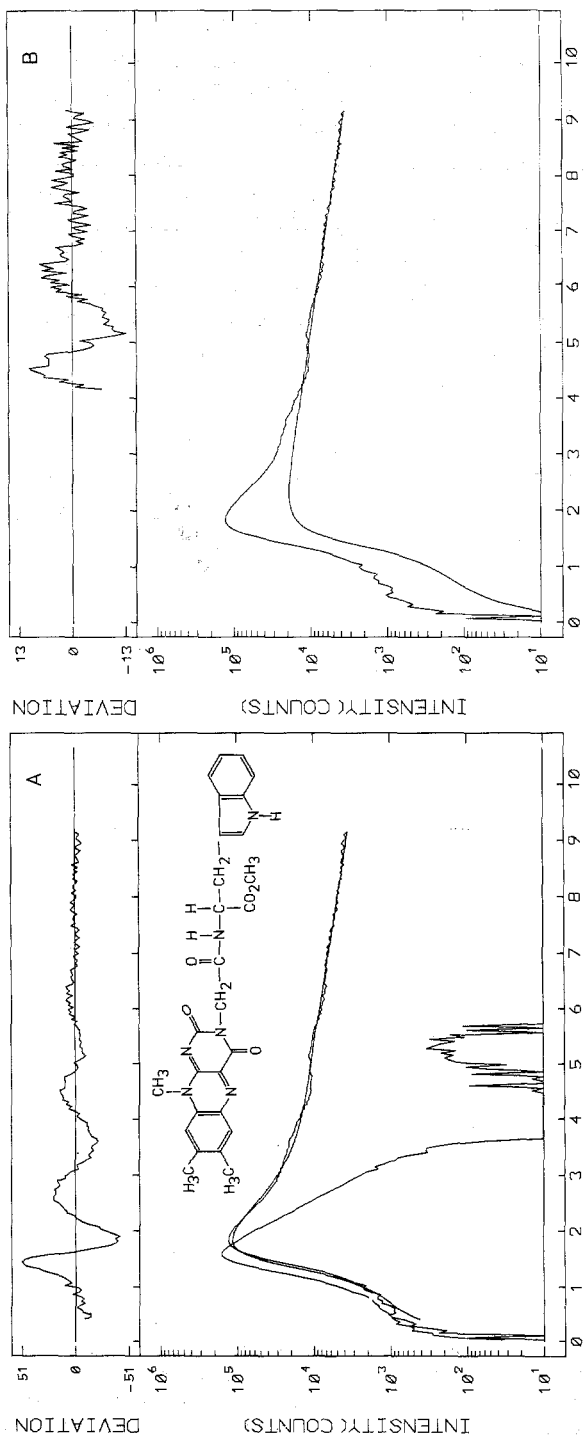

Fig. 4. Fluorescence decay curve of the flavinyltryptophan peptide in 50 mM sodium phosphate pH 7.0. Details as described in the legend of Fig. 3. A, double exponential fit of the experimental data; $\alpha_1 = 0.92$; $\tau_1 = 0.33$ ns; $\alpha_2 = 0.08$; $\tau_2 = 3.70$ ns; $\chi^2 = 200$. B, single exponential fit of the tail of the decay curve; $\tau_1 = 3.80$ ns; $\chi^2 = 23$; the convoluted curve is plotted over the entire region.

Another example of a flavin compound exhibiting a very short fluorescence lifetime is given by the flavinyltryptophan peptide. Because of the close proximity of the tryptophan residue the flavin fluorescence in the intramolecular complex is strongly quenched. The experimental results obtained with this peptide are presented in Figs. 4A and 4B. The best fit is obtained by simulating the experimental decay with a biexponential decay function. In this particular case a long lifetime component (3.7 ns) was present. Because of the short laser light-pulse repetition time (12.8 ns) a tail of the fluorescence response is present at the time that a new fluorescence event is created. This tail is the result of the response on the previous impulse and contributes to the total decay. One method to avoid this problem is to put an exponential term with the longest lifetime through the tail and subtract this contribution from the total decay curve. In this example it turned out that analysis with and without subtraction yielded nearly the same parameter values. The heterogeneity is probably due to the presence of different conformers in dynamic equilibrium. The fluorescence of the free flavin is monoexponential and has a value of 4.6 ns [4]. It should

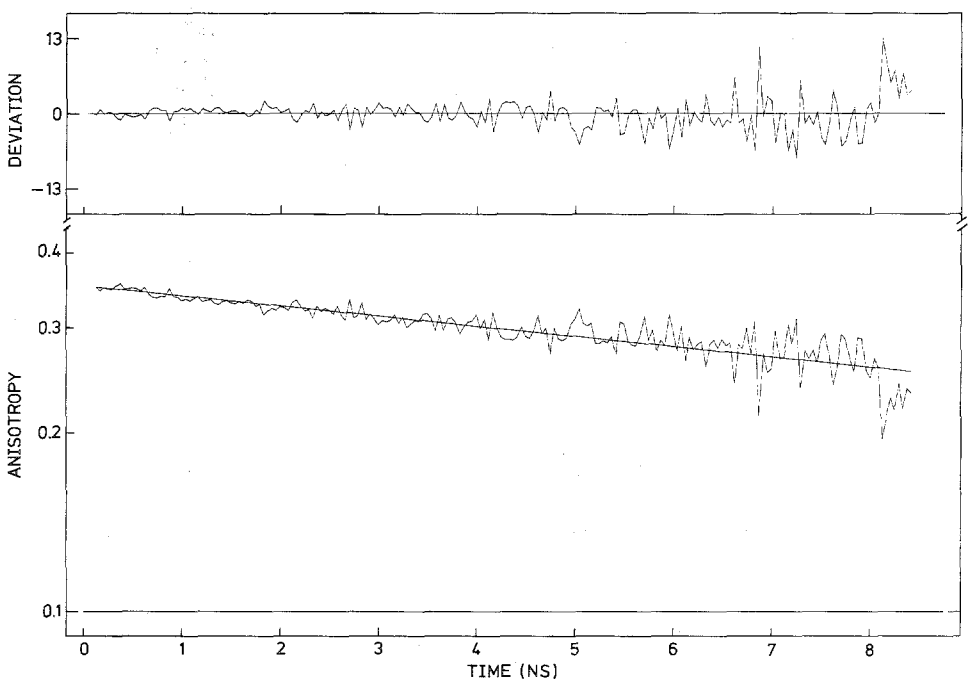

Fig. 5. Decay of emission anisotropy of FAD in lipoamide dehydrogenase. The noisy curve is the experimental anisotropy and the straight line reflects the calculated time dependence of the anisotropy with a single correlation time of 25.7 ns; $\chi^2 = 6.6 \cdot 10^{-4}$. The deviation fuction is multiplied by 10^4. The temperature was 40.0°C and the concentration of enzyme was 1 mg/ml in 30 mM sodium phosphate/0.3 mM EDTA pH 7.2.

be noted that analysis in two exponential terms leads to values less than 4.6 ns.

Decay of the emission anisotropy

Erythrosine B emission is strongly polarized due to the very short lifetime of the fluorescence. The flavin fluorescence in the dimeric flavoprotein lipoamide dehydrogenase is polarized as well, but the reason for this is that the flavin is bound rigidly to the protein, which rotates on a much slower time scale. In Fig. 5 we present the experimental decay of the emission anisotropy of the flavin in lipoamide dehydrogenase. The onset is at the maximum of the fluorescence response. The experimental data can be fitted with a single correlation time (τ_c = 25.7 ns) as is shown by the straight calculated curve and the deviation function (Fig. 5). Analysis was also performed in terms of the two models represented by equations 6 and 7. These results and other available data are collected in Table 2. Because of

TABLE 2

ANISOTROPY CHARACTERISTICS OF LIPOAMIDE DEHYDROGENASE

The results of double exponential fits of sum (S) and difference (D) decays (cf. Eqn. 3) are also presented. Conditions as given in the legend of Fig. 5.

	α_1 [a]	τ_1 [a] (ns)	α_2 [a]	τ_2 [a] (ns)	$\langle\tau\rangle$ [b] (ns)	ϕ_1 [c] (ns)	ϕ_2 [d] (ns)	ϕ_3 [e] (ns)	ϕ_4 [f] (ns)	r_0 [g]	$\langle r\rangle$ [h]
S	0.51	0.49	0.49	2.03	1.72	25.7	26.0	25.2 (22.9)	27.1	0.338	0.326
D	0.52	0.51	0.48	1.91	1.61						

[a] Symbols refer to convolution of the laser pulse with the double exponential function $\sum_{i=1}^{2} \alpha_i e^{-t/\tau_i}$, $\sum_{i=1}^{2} \alpha_i = 1$.

[b] Average lifetime defined as: $\sum_{i=1}^{2} \alpha_i \tau_i^2 / \sum_{i=1}^{2} \alpha_i \tau_i$.

[c] Correlation time obtained from one component analysis of experimental anisotropy decay.

[d] Correlation time determined from the difference curve (D) according to Eqn. 7 assuming a single time constant for motion and the lifetimes and amplitudes as determined from the total decay S.

[e] Correlation time calculated from $1/\tau_2^D - 1/\tau_2^S$ and (value between brackets) $1/\langle\tau\rangle_D - 1/\langle\tau\rangle_S$.

[f] Correlation time from the empirical formula for globular proteins [18]: $\phi_4 = (M/3.69) \cdot 10^{-3}$ ns with M = 100 000 daltons.

[g] Limiting anisotropy at time zero after the pulse (cf. Fig. 5).

[h] Steady-state emission anisotropy.

the short averaged fluorescence lifetime a single correlation time is calculated but as judged from the low χ^2 value (Fig. 5) the single time constant sufficiently reflects the motion of the bound flavin within the short observation time of 12 ns. The values in Table 2 are very close, which means that in this particular case discrimination between the two models is not possible. Also included is the strictly empirical value of the rotational correlation time for a sphere of comparable volume as for a globular protein with molecular weight of 100 000 [18].

DISCUSSION

The system as outlined is suitable for lifetimes less than 1.7 ns, since at least 99.5% of the fluorescent population is returned to the ground state after 12.8 ns (i.e. the time lapse between two laser pulses). The use of the full pulse train might lead to artifacts, especially when high radiation energies are employed or when the lifetimes are too long [14]. In the latter case the fluorescence response on the previous impulse interferes with the instantaneously excited fluorescence. Due to the improved time resolution by the use of ps laser pulses, the potential of measuring accurate biexponential decays is extended towards the subnanosecond time region. This is demonstrated in the experiment with the peptide, which exhibits a distinct heterogeneity in the fluorescence kinetics. The results can be interpreted in a way that more efficient dynamic quenching by tryptophan takes place in the conformer characterized by the shortest lifetime (0.33 ns). The other conformer (τ = 3.8 ns) corresponds with a more unfolded configuration. If in a first approximation the amplitudes are related to concentration, about 92% of the equilibrium mixture consists of the strongly quenched conformer, whereas 8% exists in a more open form. Experiments of this kind have been performed for compounds exhibiting much longer lifetimes [19]. The sensitivity of the instrumentation permits one to obtain decay curves from solutions containing even less than 10^{-10} M flavin. With these very diluted samples one has to be aware of contributions of background and impurity emission interfering with the fluorescence. An additional problem arising in flavoproteins is that the contribution of flavin released from the protein might become predominant in the fluorescence at these very low concentrations. A distinct advantage is that this system offers the possibility of direct analysis of the emission anisotropy. Using flash-lamp excitation this mode of analysis could only be applied successfully with the employment of fluorescent probes with very long lifetimes like several pyrene derivatives [20]. In the example of lipoamide dehydrogenase the FAD seems to be rigidly bound to the protein, since the correlation time obtained from the time dependence of the emission anisotropy is in good agreement with the correlation time for a spherical protein. On the other hand, one should bear in mind that the averaged fluorescence lifetime is only 1.7 ns. Such a value is rather short as compared to the much slower rotational diffusion of the protein. In

principle, with the method described one should be able to monitor faster motions localized at the site of attachment of the fluorophore.

We are currently extending the system for more versatile operation by the addition of a synchronously pumped dye laser, a frequency doubler and an extra-cavity electro-optic demodulator as pulse picker. The data collection efficiency can be doubled when the stop channel of the TAC is triggered with a 76 140 MHz signal, e.g. from another fast photodiode. These extensions improve the time resolution and expand the range of both excitation wavelengths and lifetimes.

SIMPLIFIED DESCRIPTION OF THE METHOD AND ITS APPLICATIONS

The time resolution and the sensitivity of the system used to obtain fluorescence lifetimes has been improved considerably by utilizing a mode-locked Ar ion laser as source of excitation. The ability to make time-resolved fluorescence measurements is very useful in the study of the biological and physical properties of flavins and flavoproteins as well as many other fluorescent biological molecules. The advantage of this particular system is that accurate decay curves of biological molecules with short fluorescent lifetimes and weak emissions can be obtained during a short measuring time. The experimental decay curves allow visual distinction between single and double exponential decay even in the picosecond time region. Another advantage of the employment of mode-locked laser systems coupled with fast detection electronics is that the decay of the emission anisotropy can be determined with good precision and time resolution. In this way (sub)-nanosecond time constants for rotational motion of biological molecules can be obtained directly from the experimental emission anisotropy.

ACKNOWLEDGEMENTS

We are indebted to Mr. D. Bebelaar for loan of the fast photodiode and for many helpful suggestions, to Drs. F. Müller, C. Veeger and W.H. Scouten for their interest, to Mr. B.J. Sachteleben for drawing the structural formulae and Fig. 1, and to Mrs. J.C. Toppenberg-Fang for typing. This work was supported in part by the Netherlands Foundation for Chemical Research (S.O.N.) with financial aid from the Netherlands Organization for the Advancement of Pure Research (Z.W.O.).

REFERENCES

1 Spencer, R.D. and Weber, G. (1972) in Structure and Function of Oxidation-Reduction Enzymes (Åkeson, Å, and Ehrenberg, A., eds.), pp. 393—399. Pergamon Press, Oxford
2 Visser, A.J.W.G., Li, T.M., Drickamer, H.G. and Weber, G. (1977) Biochemistry 16, 4883—4886
3 Wahl, Ph., Auchet, J.C., Visser, A.J.W.G. and Müller, F. (1974) FEBS Lett. 44, 67—70
4 Visser, A.J.W.G. and Müller, F. (1979) Helv. Chim. Acta 62, 593—608
5 Mackenzie, R.E., Föry, W. and McCormick, D.B. (1969) Biochemistry 8, 1839—1844
6 Visser, A.J.W.G., Grande, H.J., Müller, F. and Veeger, C. (1974) Eur. J. Biochem. 45, 99—107

7 Grande, H.J., van Schagen, C.G., Jarbandhan, T. and Müller, F. (1977) Helv. Chim. Acta 60, 348—366
8 Föry, W., Mackenzie, R.E. and McCormick, D.B. (1968) J. Heterocyclic Chem. 5, 625—630
9 Massey, V., Gibson, Q.H. and Veeger, C. (1960) Biochem. J. 77, 341—351
10 Spears, K.G., Cramer, L.E. and Hoffland, L.D. (1978) Rev. Sci. Instrum. 49, 255—262
11 Spencer, R.D. and Weber, G. (1970) J. Chem. Phys. 52, 1654—1663
12 Grinvald, A. and Steinberg, I.Z. (1974) Anal. Biochem. 59, 583—598
13 Wahl, Ph., Auchet, J.C. and Donzel, B. (1974) Rev. Sci. Instrum. 45, 28—32
14 Eisenthal, K.B. (1977) Annu. Rev. Phys. Chem. 28, 207—232
15 Dale, R.E., Chen, L.A. and Brand, L. (1977) J. Biol. Chem. 252, 7500—7510
16 Blumberg, W.E., Dale, R.E., Eisinger, J. and Zuckerman, D.M. (1974) Biopolymers 13, 1607—1620
17 Easter, J.H., DeToma, R.P. and Brand, L. (1976) Biophys. J. 16, 571—583
18 Chen, R.F. (1967) in Fluorescence: Theory, Instrumentation and Practice (Guilbault, G., ed.), p. 469. Marcel Dekker, New York
19 Donzel, B., Gauduchon, P. and Wahl, Ph. (1974) J. Am. Chem. Soc. 96, 801—808
20 Lovejoy, C., Holowka, D.A. and Cathou, R.E. (1977) Biochemistry 16, 3668—3672